Journal of the Serbian Chemical Society
JSCS@tmf.bg.ac.rs • www.shd.org.rs/JSCS
J. Serb. Chem. Soc. *88* (12) 1253–1264 (2023)
JSCS–5693
Original scientific paper
Published 19 December 2023

Synthesis and structural analysis of tetranuclear Zn(II) complex with 2,3-dihydroxybenzaldehyde-aminoguanidine

MARIJANA S. KOSTIĆ[#], MARKO V. RODIĆ*[#], LJILJANA S. VOJINOVIĆ-JEŠIĆ[#] and MIRJANA M. RADANOVIĆ[#]

University of Novi Sad, Faculty of Sciences, Trg Dositeja Obradovića 3, 21000, Novi Sad

(Received 8 August, revised 22 August, accepted 8 September 2023)

Abstract: Here we report a new Schiff base of aminoguanidine and 2,3-dihydroxybenzaldehyde (H_2L) and its physicochemical characterization, along with an investigation into its coordination affinities towards zinc. By reacting zinc acetate with the chloride salt of the ligand in the MeCN–H_2O solution, yellow single-crystals of tetranuclear, centrosymmetric complex, with the formula $[Zn_2(\mu\text{-}L)(\mu\text{-}OAc)_2]_2 \cdot 2MeCN$, were obtained. The complex was characterized by IR spectroscopy, conductometry, elemental analysis, and single-crystal X-ray diffraction analysis. Notably, both nitrogen atoms of the aminoguanidine residue coordinate to the same zinc atom, while both deprotonated phenyl oxygen atoms achieve bridging coordination. Furthermore, two acetate anions bridge adjacent zinc atoms in addition to the Schiff base anion. Meaningful insights into the hierarchy and significance of intermolecular interactions within the crystal structure were gained by estimating the energies using the CrystalExplorer model. The calculations revealed that the crystal structure can be classified as a layer type, with notably stronger interactions occurring along the [001] and [011] directions.

Keywords: Schiff base; guanylhydrazones; acetate coordination; crystal structure.

INTRODUCTION

Schiff bases and their metal complexes represent a large class of compounds interesting from both fundamental and practical points of view,[1] due to their easy synthesis, versatile structural features, and coordination modes, but also the enormous application potential in many different fields. Some of these compounds are good analytical and electroanalytical reagents, precursors in organic synthesis, catalysts, polymer stabilators, *etc*.[2] On the other hand, the others show promising anti-tuberculosis, antimicrobial, anti-inflammatory, and antitumor activities.[3] Additionally, an interest in Schiff bases and their metal complexes and

* Corresponding author. E-mail: marko.rodic@dh.uns.ac.rs
https://doi.org/10.2298/JSC230808067K

their use as organic layers in OLED materials and other emissive organic devices,[4] as well as photosensitizers in dye-sensitized solar cells,[5] has arisen. The steric, electronic and biological potential of the mentioned compounds is tunable by choosing the appropriate amine and carbonyl precursors. One of the always interesting areas of coordination chemistry is the design of novel Schiff bases, especially those with multiple donor sites.[6] Having that in mind, the Schiff bases of 2,3-dihydroxybenzaldehyde seem to be a worthwhile candidate for further research.[7,8]

Zinc is well known for its biocompatibility and versatile importance for the organism.[6] However, the interest in phenoxido-bridged complexes of metals of group 12 was not great, mainly due to the absence of magnetic interactions.[9] Nevertheless, the fact that group 12 metal complexes usually show high photoluminescence, made them interesting for research in the field of optoelectronic devices.[10,11]

Based on the aforementioned, the presented research was designed to gain better insight into the coordination properties of the Schiff bases of aminoguanidine, obtain a phenoxido-bridged complex and characterize it. The Schiff base of aminoguanidine and 2,3-dihydroxybenzaldehyde and its first complex, *viz.* $[Zn_2(\mu\text{-L})(\mu\text{-OAc})_2]_2 \cdot 2MeCN$ are synthesized and physicochemically characterized. The structure of this tetranuclear centrosymmetric complex was determined by SC-XRD, and thoroughly discussed.

EXPERIMENTAL

Reagents

All chemicals used for syntheses and characterization were reagent-grade and used as received from commercial sources, without further purification.

Preparation of the ligand L·HCl – 2,3-dihydroxybenzaldehyde-aminoguanidine hydrogenchloride

2,3-Dihydroxybenzaldehide (25 mmol, 3.45 g) was dissolved in 75 mL H_2O, and 25 mmol (2.75 g) of aminoguanidine hydrogenchloride was added. The resulting mixture was refluxed for 1.5 h during which it completely dissolves. The resulting yellow solution was left at room temperature. After seven days, the yellow product was filtered and washed with H_2O. Yield: 3.50 g (67 %).

Preparation of $[Zn_2(\mu\text{-L})(\mu\text{-OAc})_2]_2 \cdot 2MeCN$

A mixture of 0.5 mmol (0.128 g) of the obtained ligand and 0.5 mmol (0.092 g) $Zn(OAc)_2 \cdot 2H_2O$ was poured over with 6 mL of CH_3CN–H_2O mixture (1:1), heated slightly until dissolved, and the resulting yellow solution was left at room temperature. After two days, yellow prismatic single crystals were filtered and washed with CH_3CN. Yield: 0.088 g (30 %).

Analytical methods

The air-dried compounds were subjected to elemental analyses (C, H, N) using standard micro-methods. Molar conductivity measurements of freshly prepared solutions (c = 1 mmol L^{-1}) were performed on a Jenway 4010 conductivity meter. The IR spectra were recorded on a

Nicolet Nexus 670 FTIR (Thermo Scientific) spectrophotometer in the 400–4000 cm^{-1} range by the KBr pellet technique. Melting points were determined using a Nagema melting point microscope Rapido.

Analytical and spectral data of the synthesized compounds are given in Supplementary material to this paper.

Crystal structure determination

X-ray diffraction data were obtained from a suitable single crystal using an Oxford Diffraction Gemini S diffractometer. The probe used was a graphite-monochromated MoKα X-radiation from a sealed tube. Reflections were recorded on a Sapphire CCD area detector at room temperature. CrysAlisPro was employed for instrument control and raw frames processing.[12] The crystal structure was solved using SHELXT[13] and refined with SHELXL.[14] For graphical user interface, ShelXle was utilized.[15]

During refinement, all non-hydrogen atoms were assigned anisotropic displacement parameters. Carbon-bonded hydrogen atoms were positioned ideally according to parent atom stereochemistry and refined using a riding model with their displacement parameters assumed to be a suitable multiple of the carrier atom's U_{eq}. Nitrogen-bonded hydrogen atoms were identified through residual density maps in the final iterations of the refinement. Their positions were refined with distance restraints, and their displacement parameters were treated similarly to those of hydrogen atoms bonded to carbons. Details are listed in Table S-I of the Supplementary material.

The crystal structure was internally validated using Platon[16] and externally validated against structures with similar fragments in the Cambridge Structural Database (CSD)[17] through the Mogul algorithm[18] implemented in the Mercury CSD.[19]

Interaction energies calculations

Intermolecular energy calculations were employed to examine the crystal packing using CrystalExplorer.[20] Quantum chemistry calculations were performed using TONTO[21] as the backend. A Hirshfeld surface was computed for the complex molecule, and all nearby molecules were taken into account for the pairwise energy calculations. CE-HF model energies were employed.[22]

RESULTS AND DISCUSSION

Syntheses and characterization

Yellow microcrystals of the ligand were obtained in the reaction of an aqueous solution 2,3-dihydroxybenzaldehyde and aminoguanidine hydrogenchloride in a mole ratio of 1:1 under reflux conditions. Subsequently, the obtained ligand was reacted with zinc(II) acetate, in a 1:1 mole ratio in a MeCN–H_2O solution, resulting in the formation of prismatic yellow single crystals of neutral Zn(II) complex of the formula $[Zn_2(\mu\text{-L})(\mu\text{-OAc})_2]_2 \cdot 2MeCN$.

Obtained ligand is well soluble in water, methanol, ethanol, acetonitrile, and dimethylformamide. The complex is well soluble in dimethylformamide, moderately soluble in acetone and methanol, and only sparingly soluble in water, ethanol and acetonitrile. The molar conductivity value of the complex dissolved in DMF (8 S cm^2 mol^{-1}) confirms its non-electrolyte nature.

The ligand is coordinated in its dianionic form as N_2O_2 tetradentate, involving coordination through azomethine and imino nitrogen atoms, and phenolic oxygen atoms. This is primarily assumed by the comparison of the IR spectrum of the complexes with that of the ligand. In the spectrum of the complex, the bands related to the ν(C–N) vibrations in the guanido fragment, as well as the band originating from the azomethine function, display a negative shift of approximately 50 cm^{-1}. Furthermore, the ν(Ar–O) band, present at 1264 cm^{-1} in the ligand's spectrum, experiences a shift to 1250 cm^{-1} in the spectrum of the complex, suggesting coordination of the phenolic oxygen atom.[23] Bands in the region 3600–3000 cm^{-1}, originating from O–H vibrations in the spectrum of the ligand, are absent in the complex' spectrum, indicative of ligand deprotonation. Additionally, bands in the 1460–1400 cm^{-1} region are potentially attributed to ν(O–Ac) vibrations of coordinated acetate ions,[24] although this assignment is challenging due to the presence of numerous other bands in this spectral region in the IR spectrum of the uncomplexed ligand.

Crystal structure description

The molecular structure of the obtained tetranuclear Zn(II) complex is presented in Fig. 1 and key structural data are presented in Table I. The asymmetric unit contains the dianion of the chelate ligand, which is coordinated as ONN tridentate to one zinc atom (Zn1) and monodentate *via* the oxygen atom of the deprotonated hydroxyl group from position 3 to the second zinc atom (Zn2). Additionally, two acetate ions bridge two adjacent units, and a solvent molecule is also present.

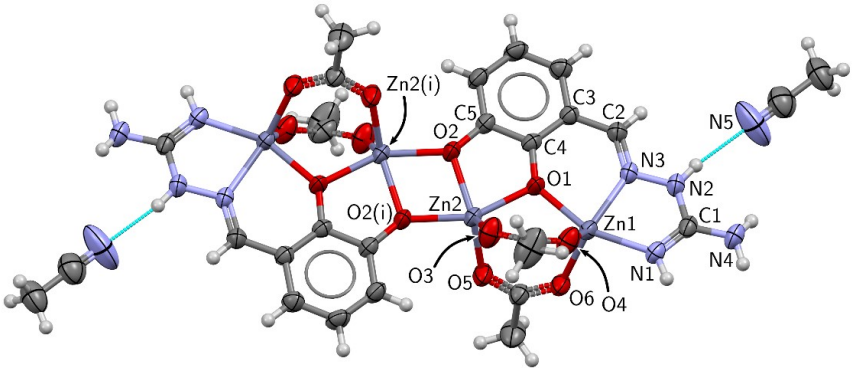

Fig. 1. Molecular structure of the complex formula $[Zn_2(\mu\text{-L})(\mu\text{-OAc})_2]_2 \cdot 2MeCN$. Symmetry operation: (*i*) $-x+1, -y+1, -z$.

The coordination mode of the chelating ligand in this centrosymmetric complex is intriguing and multifaceted. The chelating ligand employs four donor

atoms for coordination (N_2O_2), namely, azomethine and imino nitrogen atoms, and two phenolic oxygen atoms as donors. Both oxygen atoms have a bridging role connecting two zinc atoms. The tridentate ONN coordination of the chelating ligand was achieved through the oxygen atom of the deprotonated hydroxyl group from position 2, and nitrogen atoms from azomethine and imino group from aminoguanidine residue. Except through acetate bridges, neighboring units are connected by bridging coordination of oxygen atoms O1 and O2. The resulting intermetallic distances are 3.3008(4) and 3.1926(4) Å for Zn1···Zn2 and Zn2···Zn2^i, respectively (symmetry operation: (i) $-x+1, -y+1, -z$).

TABLE I. Selected bond lengths and valence angles; symmetry operation: (i) $-x+1, -y+1, -z$

Bond	Bond length, Å	Bonds	Bond angle, °
Zn1–N1	2.024(2)	N1–Zn1–N3	76.12(7)
Zn1–N3	2.183(2)	N1–Zn1–O1	157.36(7)
Zn1–O1	1.993(2)	N3–Zn1–O1	81.36(7)
Zn1–O4	2.013(2)	N3–Zn1–O4	130.30(7)
Zn1-O6	2.033(2)	N3–Zn1–O6	124.41(7)
Zn2–O1	2.053(2)	O1–Zn2–O2	153.86(6)
Zn2–O2	2.007(2)	O1–Zn2–O3	96.99(7)
Zn2–O2^i	2.007(2)	O1–Zn2–O5	94.82(7)
Zn2–O3	1.983(2)	O2–Zn2–O2^i	75.72(6)
Zn2–O5	2.001(1)	O2–Zn2–O3	100.24(7)
Zn1···Zn2	3.3008(4)	O2^i–Zn2–O3	123.28(7)
Zn2···Zn2^i	3.1926(4)	O2–Zn2–O5	98.48(7)
N1–C1	1.293(3)	O2^i–Zn2–O5	129.04(7)
N2–C1	1.357(3)	O3–Zn2–O5	107.64(7)
N3–C2	1.281(3)	N1–C1–N2	118.4(2)
N4–C1	1.350(3)	N1–C1–N4	126.9(2)
C2–C3	1.440(3)	O3–C10–O4	126.6(2)
O1–C4	1.329(2)	O5–C11–O6	126.1(2)
O2–C5	1.333(3)	Bonds	Torsion angle, °
O3–C10	1.248(3)	N1–C1–N2–N3	0.3(3)
O4–C10	1.244(3)	N4–C1–N2–N3	−178.5(2)
O5–C11	1.245(3)	C1–N2–N3–C2	176.4(2)
O6–C11	1.257(3)	N2–N3–C2–C3	−179.4(4)

This coordination of the chelate ligand and acetate ions as coligands to four zinc atoms resulted in the formation of a diverse array of versatile metallocycles. These include four five-membered and two six-membered chelate rings with one metal atom, along with one four-membered, four six-membered, and two eight--membered metallocycles with two metal atoms. All rings containing one metal atom are essentially flat. Of those with two metal atoms, the four-membered ring is planar due to symmetry restriction, while others are significantly puckered.

In this complex, Zn(II) ions, denoted as Zn1 and Zn2, adopt highly deformed N_2O_3 and O_5 environments, respectively. The results obtained from Addison's method[25] and Holmes' method[26–28] show differences in assessing whether the polyhedra centered at Zn1 and Zn2 are closer to the ideal square pyramid with a trans basal angle of 150° (SPY-5) or the ideal trigonal bipyramid (TBPY-5).

In particular, based on the τ_5 values (τ_5 = 0.45 for Zn1 and τ_5 = 0.41 for Zn2), both polyhedra are determined to be closer to SPY-5 than TBPY-5. However, Holmes' method places both polyhedra at 36 % along the Berry pseudorotation coordinate $D_{3h}\rightarrow C_{2v}\rightarrow C_{4v}$. This suggests a closer proximity to TBPY-5, but it also indicates significant deviations from the ideal Berry pseudorotation in both cases.

This later outcome is consistent with the calculations of continuous shape measures,[29] which assign both polyhedrons a closer alignment to TBPY-5 (*S*(TBPY-5) = 2.147 for Zn1; *S*(TBPY-5) = 2.301 for Zn2) than to SPY-5 (*S*(SPY-5) = 3.444 for Zn1; *S*(SPY-5) = 3.255 for Zn2). However, both deformation paths diverge by 42 % from the ideal Berry pseudorotation coordinate which represents minimal distortion pathway in this polyhedral rearrangement.[30]

The coordination environment of Zn1 formally adopts a trigonal-bipyramidal configuration, with the axial positions being occupied by the N1 and O1 atoms of the Schiff base ligand. This arrangement is supplemented by the presence of N3 from the Schiff base ligand, in addition to two oxygen atoms (O4 and O6) derived from bridging acetate ions, collectively constituting the equatorial plane. On the other hand, Zn2 also adopts a trigonal-bipyramidal coordination. In this context, the equatorial plane is formed by the participation of two oxygen atoms (O3 and O5) originating from acetate bridges, along with an O2 moiety sourced from a 2,3-dihydroxybenzaldehyde fragment located in an adjacent subunit. Meanwhile, the axial positions are occupied by the hydroxyl groups of 2,3-dihydroxybenzaldehyde, namely O2 and O1, the latter stemming from the neighboring subunit.

Atom Zn1 forms the longest bond with the N3 donor atom of the azomethine group, and the shortest one with the O1 ligator from the hydroxyl group of 2,3--dihydroxybenzaldehyde. On the other hand, Zn2 forms the longest Zn2–ligand bond with the bridging O1 atom, while the shortest bond is between Zn2 and O3 from the carboxyl group of the acetato ligand. The second oxygen atom from this carboxyl group (O4) forms a slightly longer bond with the first zinc atom, Zn1.

In the aminoguanidine fragment of the ligand, the C2–N3 and C1–N1 bond lengths indicate the presence of localized double bonds, whereas the other bonds in this fragment exhibit intermediate lengths, which can be attributed to electron delocalization, a common feature for this class of compounds.[31] In the 2,3-dihydroxybenzaldehyde part of the chelating ligand, the longest bond observed is C2–C3, which is the bond between the carbon atom of the benzene ring and the carbon

atom of the azomethine group. Remarkably, this C2–C3 bond stands as the longest bond within the entire ligand structure.

Another intriguing feature of this structure is the exo-bidentate coordination of two acetate ligands. The survey of CSD[17] was made to gain further insight into the prevalence of this coordination mode and similar ones involving acetate ligands. The survey revealed that the bridging mode of coordination of two acetate ions in zinc(II) complexes was found in 240 structures. In most instances, these complexes are binuclear, featuring (bis)condensed carbonyl compounds or monodentate ligands. The occurrence of polynuclear complexes with this specific coordination mode of acetate ions is relatively less frequent.

Although the coordination mode presented here is complex, it is not unexpected. It showcases an interesting attribute of the 2,3-dihydroxybenzaldehyde fragment when acetate serves as a bridging coligand, as exemplified in the structure of the tetranuclear complex described in the work.[32]

Upon inspection of the Hirshfeld surface of the complex molecule, 22 nearest neighbors (11 independent pairs) can be identified within the crystal structure. The results of pairwise intermolecular interaction energies calculation are given in Table II. Among these neighbors, 16 are complex molecules, forming 8 independent pairs. Notably, the crystal packing energy landscape is dominated by two pairs, with interaction energies exceeding 100 kJ mol^{-1}. Furthermore, only two more pairs were found to have energy contributions surpassing 15 kJ mol^{-1}.

TABLE II. Summary of important intermolecular interaction energies in the crystal structure of $[Zn_2(\mu\text{-L})(\mu\text{-OAc})_2]_2\cdot 2MeCN$; R is the distance between molecular centroids. $E_{tot} = k_{ele}E_{ele} + k_{pol}E_{pol} + k_{dis}E_{dis} + k_{rep}E_{rep}$, where scale factors for benchmarked CE-HF energy model are $k_{ele} = 1.019$, $k_{pol} = 0.651$, $k_{dis} = 0.901$, and $k_{rep} = 0.811$, as taken from the paper of Thomas *et al.*[33] Symmetry operation correspond to the second molecule in the pair

Label	N	Symmetry operation	R / Å	E / kJ mol^{-1}				
				E_{ele}	E_{pol}	E_{dis}	E_{rep}	E_{tot}
Complex⋯ Complex								
I	2	Translation	15.50	−115.8	−36.9	−41.0	0.0	−178.9
II	2	Translation	11.44	−80.5	−32.2	−82.3	28.6	−153.9
III	2	Translation	9.99	1.6	−14.0	−56.2	27.0	−36.2
IV	2	Translation	8.82	7.4	−10.4	−45.7	18.9	−25.2
V	2	Translation	16.62	−12.4	−2.8	−5.0	0.0	−18.9
VI	2	Translation	14.65	−3.2	−0.8	−5.1	0.0	−8.4
VII	2	Translation	14.61	3.8	−0.6	−5.6	0.0	−1.6
VIII	2	Translation	11.91	10.1	−1.3	−10.5	2.3	1.8
Complex⋯MeCN								
IX	2	Translation	10.68	−59.5	−16.8	−8.6	44.7	−43.1
X	2	Inversion	6.53	−24.4	−4.8	−25.6	10.6	−42.5
XI	2	Inversion	3.60	−12.2	−10.5	−35.2	17.2	−37.0

The strongest intermolecular interaction observed in the crystal structure (–179 kJ mol^{-1}) occurs between complex molecules related by translation (for symmetry codes see Table II). This interaction is predominantly driven by electrostatic forces, which can be attributed to the excellent complementarity in molecular electrostatic potential on the patches of the Hirshfeld surfaces of neighboring molecules (Fig. 2a). The interaction is mediated through N4–H4B···O6(i) hydrogen bond (d(N4–H4B) = 0.853(16) Å, d(H4B···O6(i)) = = 2.154(17) Å, d(N4··· O6(i)) = 2.981(2) Å and α(N4–H4B···O6(i)) = 163(2)°; symmetry operation: (*i*) x, y+1, z+1). Due to centrosymmetric nature of the complex molecule, these interactions occur in pairs, combining to create a 24-membered ring with graph set descriptor $R_2^2(24)$.[34] These interactions then form a chain, that propagates in the [011] direction.

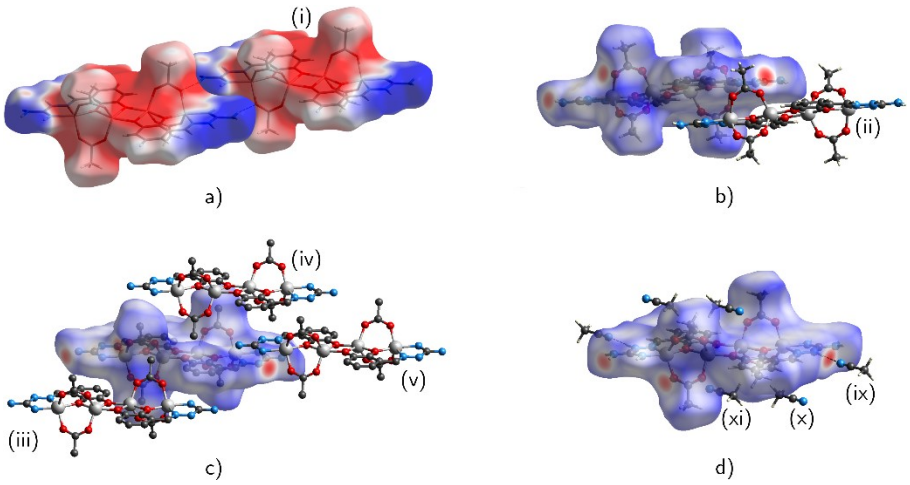

Fig. 2. a) Hirshfeld surfaces of the molecular pair of $[Zn_2(\mu\text{-L})(\mu\text{-OAc})_2]_2$ with strongest interaction, decorated with molecular electrostatic potential in the range from −0.05 a.u. (red) to +0.05 a.u. (blue); b)–d) selected molecules surrounding a central one of $[Zn_2(\mu\text{-L})(\mu\text{-OAc})_2]_2$ with its Hirshfeld surface decorated with d_{norm}. Molecules are labeled as in Table II.

The second strongest interaction (−153 kJ mol^{-1}) has equal contribution of dispersion and electrostatic components, as well as a non-negligible contribution from polarization effects. Notably, no significant atom–atom short contacts can be identified (Fig. 2b), and the detection of this interaction is a direct consequence of the whole-molecule approach to the crystal packing analysis, rather than focusing solely on atom–atom features. These interactions form a chain that propagates along the crystallographic axis *c*.

Only three more interactions are noteworthy (Fig. 2c), as the weakest two make minor contributions to the lattice energy. Specifically, two independent pairs exhibit interaction energies of −36 and −25 kJ mol^{-1}, dominated solely by dispersion forces, with a minor contribution from polarization terms. Interestingly, electrostatic contribution is slightly destabilizing for these interactions. The third pair represents the final one with a notable interaction energy (−19 kJ mol^{-1}), which is predominantly governed by electrostatics. However, due to the considerable separation between the molecules (Cg···Cg distance of 16.6 Å), the interaction is relatively weak. Notably, all three mentioned cases exhibit no significant atom–atom short contacts between the molecules involved.

Surrounding each complex molecule are six MeCN molecules, forming three independent pairs. Only one pair is involved in a hydrogen bond N2–H2···N5 (d(N2–H2) = 0.84(2)Å, d(H2···N5) = 2.04(2)Å, d(N2···N5) = 2.872(5) Å, α(N2–H2···N5) = 169(2)°) with an interaction energy of −43 kJ mol^{-1}, predominantly governed by electrostatic forces. The other two independent pairs have comparable interaction energies (−43 and −37 kJ mol^{-1}), with a significant contribution from dispersion forces and no notable atom–atom short contacts (Fig. 2d).

Overall, from the perspective of energy of the intermolecular interactions, crystal structure can be classified as a layer type, as depicted by an energy framework shown in Fig. 3. Notably, significantly stronger interactions occur along the [001] and [011] directions, with a higher proportion of electrostatic contributions, leading to the observed anisotropy in their distribution.

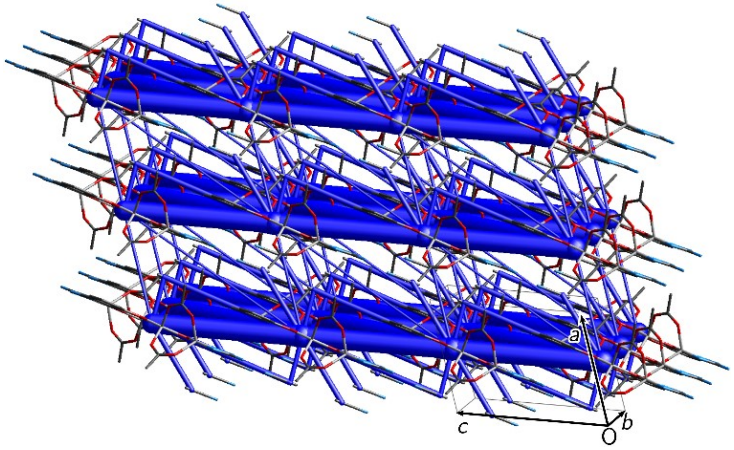

Fig. 3. Energy framework for the crystal structure of [Zn_2(μ-L)(μ-OAc)$_2$]$_2$·2MeCN, represented in a 3×3×3 cells cluster. Total interaction energy is proportional to blue tubes diameter. Only interactions with $-E$ < 15 kJ mol^{-1} are displayed.

CONCLUSION

The yellow microcrystals of the ligand were obtained in the reaction of an aqueous solution 2,3-dihydroxybenzaldehyde and aminoguanidine hydrogenchloride in a mole ratio of 1:1 under reflux conditions, and characterized by IR spectroscopy and elemental analysis. The reaction of the obtained ligand and zinc acetate yielded the formation of yellow single crystals of the tetranuclear complex $[Zn_2(\mu\text{-L})(\mu\text{-OAc})_2]_2\cdot 2MeCN$. This is the first complex with the obtained Schiff base, as well as the first tetranuclear complex with aminoguanidine derivatives. The SC-XRD revealed an interesting coordination mode with two nitrogen and two oxygen atoms of the chelating ligand involved in coordination, with the latter being the bridging ligators, as well. Besides, bidentate bridging coordination of four acetate ions was found. The hierarchy and significance of intermolecular interactions within the crystal structure were calculated and those results showed the crystal structure could be classified as a layer type, with notably stronger interactions occurring along the [001] and [011] directions. The detailed knowledge of the crystal structure and intermolecular interactions present is vital for the design of further research, which is currently being done concerning the optical characteristics, as well as the antioxidant activity of these compounds.

SUPPLEMENTARY MATERIAL

Additional data and information are available electronically at the pages of journal website: https://www.shd-pub.org.rs/index.php/JSCS/article/view/12533, or from the corresponding author on request. CCDC 2285370 contains the supplementary crystallographic data for this paper. These data can be obtained free of charge from The Cambridge Crystallographic Data Centre (https://www.ccdc.cam.ac.uk/structures).

Acknowledgement. The authors gratefully acknowledge the financial support of the Ministry of Science, Technological Development and Innovation of the Republic of Serbia (Grant No. 451-03-47/2023-01/200125).

ИЗВОД

СИНТЕЗА И СТРУКТУРНА АНАЛИЗА ТЕТРАНУКЛЕАРНОГ КОМПЛЕКСА Zn(II) СА 2,3-ДИХИРОКСИБЕНЗАЛДЕХИД-АМИНОГВАНИДИНОМ

МАРИЈАНА С. КОСТИЋ, МАРКО В. РОДИЋ, ЉИЉАНА С. ВОЈИНОВИЋ ЈЕШИЋ и МИРЈАНА М. РАДАНОВИЋ

Универзитет у Новом Саду, Природно-математички факултет, Трг Доситеја Обрадовића 3, 21000 Нови Сад

У овом раду приказана је синтеза и физичкохемијска карактеризација нове Шифове базе аминогванидина и 2,3-дихидроксибензалдехида, као и испитивање координационих својстава добијеног једињења. У реакцији цинк-ацетата и хлоридне соли лиганда у смеши растварача ацетонитрил-вода добијени су жути монокристали тетрануклеарног, центросиметричног комплекса формуле $[Zn_2(\mu\text{-L})(\mu\text{-OAc})_2]_2\cdot 2MeCN$. Комплекс је окарактерисан ИС спектроскопијом, кондуктометријом, елементалном анализом и рендгенском структурном анализом. У добијеном комплексу, оба донорна атома азота аминогванидинског фрагмента координовани су за исти атом цинка, док оба атома кисеоника депротонованих фенолних група имају улогу моста. Осим тога, ацетатни јони

такође остварују мостовну координацију. Испитивање значајних међумолекулских интеракција извршено је проценом енергија уз коришћење CrystalExplorer модела. На основу ових прорачуна може се закључити да се кристална структура може сматрати слојевитом, са значајно јачим интеракцијама дуж [001] и [011] праваца.

(Примљено 8. августа, ревидирано 22. августа, прихваћено 18. септембра 2023)

REFERENCES

1. D. Aggoun, Z. Messasma, B. Bouzerafa, R. Berenguer, E. Morallon, Y. Ouennoughi, A. Ourari, *J. Mol. Struct.* **1231** (2021) 129923 (https://doi.org/10.1016/J.MOLSTRUC.2021.129923)
2. A. Kajal, S. Bala, S. Kamboj, N. Sharma, V. Saini, *Journal of Catalysts* **2013** (2013) 1 (https://doi.org/10.1155/2013/893512)
3. Saswati, M. Mohanty, A. Banerjee, S. Biswal, A. Horn, G. Schenk, K. Brzezinski, E. Sinn, H. Reuter, R. Dinda, *J. Inorg. Biochem.* **203** (2020) 110908 (https://doi.org/10.1016/J.JINORGBIO.2019.110908)
4. M. Barwiolek, D. Jankowska, M. Chorobinski, A. Kaczmarek-Kędziera, I. Łakomska, S. Wojtulewski, T. M. Muzioł, *RSC Adv.* **11** (2021) 24515 (https://doi.org/10.1039/D1RA03096E)
5. P. Mahadevi, S. Sumathi, *Synth. Commun.* **50** (2020) 2237 (https://doi.org/10.1080/00397911.2020.1748200)
6. H. Kargar, M. Fallah-Mehrjardi, R. Behjatmanesh-Ardakani, H. A. Rudbari, A. A. Ardakani, S. Sedighi-Khavidak, K. S. Munawar, M. Ashfaq, M. N. Tahir, *Inorg. Chim. Acta* **530** (2022) 120677 (https://doi.org/10.1016/J.ICA.2021.120677)
7. M. Martínez Belmonte, E. C. Escudero-Adán, E. Martin, A. W. Kleij, *Dalton Transactions* **41** (2012) 5193 (https://doi.org/10.1039/C2DT30201B)
8. B. B. Tang, H. Ma, G. Z. Li, Y. B. Wang, G. Anwar, R. Shi, H. Li, *CrystEngComm* **15** (2013) 8069 (https://doi.org/10.1039/C3CE41034J)
9. R. Biswas, C. Diaz, A. Ghosh, *Polyhedron* **56** (2013) 172 (https://doi.org/10.1016/J.POLY.2013.03.046)
10. J. Adhikary, P. Chakraborty, S. Samanta, E. Zangrando, S. Ghosh, D. Das, *Spectrochim. Acta A Mol Biomol Spectrosc* **178** (2017) 114 (https://doi.org/10.1016/j.saa.2017.01.041)
11. B. Babic, M. Romcevic, M. Gilic, J. Trajic, M. M. Radanović, L. S. Vojinović-Ješić, M. V. Rodić, N. Romcevic, *Opt. Mater. (Amst)* **136** (2023) 113445 (https://doi.org/10.1016/J.OPTMAT.2023.113445)
12. Rigaku Oxford Diffraction, *CrysAlisPro Software system*, Rigaku Corporation, Oxford, 2022
13. G. M. Sheldrick, *Acta Cryst., A* **71** (2015) 3 (https://doi.org/10.1107/S2053273314026370)
14. G. M. Sheldrick, *Acta Cryst. C Struct. Chem.* **71** (2015) 3 (https://doi.org/10.1107/S2053229614024218)
15. C. B. Hübschle, G. M. Sheldrick, B. Dittrich, *J. Appl. Cryst.* **44** (2011) 1281 (https://doi.org/10.1107/S0021889811043202)
16. A. L. Spek, *Acta Cryst. D Biol Cryst.* **65** (2009) 148 (https://doi.org/10.1107/S090744490804362X)
17. C. R. Groom, I. J. Bruno, M. P. Lightfoot, S. C. Ward, *Acta Cryst., B* **72** (2016) 171 (https://doi.org/10.1107/S2052520616003954)

18. I. J. Bruno, J. C. Cole, M. Kessler, J. Luo, W. D. S. Momerwell, L. H. Purkis, B. R. Smith, R. Taylor, R. I. Cooper, S. E. Harris, A. G. Orpen, *J. Chem. Inf. Comp. Sci.* **44** (2004) 2133 (https://doi.org/10.1021/CI049780B)
19. C. F. MacRae, I. Sovago, S. J. Cottrell, P. T. A. Galek, P. McCabe, E. Pidcock, M. Platings, G. P. Shields, J. S. Stevens, M. Towler, P. A. Wood, *J. Appl. Cryst.* **53** (2020) 226 (https://doi.org/10.1107/S1600576719014092)
20. P. R. Spackman, M. J. Turner, J. J. McKinnon, S. K. Wolff, D. J. Grimwood, D. Jayatilaka, M. A. Spackman, *J. Appl. Cryst.* **54** (2021) 1006 (https://doi.org/10.1107/S1600576721002910)
21. D. Jayatilaka, D. J. Grimwood, in *Computational Science — ICCS 2003. ICCS 2003. Lecture Notes in Computer Science*, P. M. A. Sloot, D. Abramson, A. V. Bogdanov, Y. E. Gorbachev, J. J. Z. A. Y. Dongarra, Eds., Springer, Berlin, 2003
22. S. P. Thomas, P. R. Spackman, D. Jayatilaka, M. A. Spackman, *J. Chem. Theor. Comput.* **14** (2018) 1614 (https://doi.org/https://doi.org/10.1021/acs.jctc.7b01200)
23. W. K. Dong, J. Zhang, Y. Zhang, N. Li, *Inorg. Chim. Acta* **444** (2016) 95 (https://doi.org/10.1016/J.ICA.2016.01.034)
24. K. Nakamoto, *Infrared and Raman spectra of inorganic and coordination compounds. Part B, Applications in coordination, organometallic, and bioinorganic chemistry*, Wiley, New York, 2009
25. A. W. Addison, T. N. Rao, J. Reedijk, J. van Rijn, G. C. Verschoor, *J. Chem. Soc., Dalton Trans.* (1984) 1349 (https://doi.org/10.1039/DT9840001349)
26. R. R. Holmes, J. A. Deiters, *J. Am. Chem. Soc.* **99** (1977) 3318 (https://doi.org/10.1021/ja00452a021)
27. R. R. Holmes, *Acc. Chem. Res.* **12** (1979) 257 (https://doi.org/10.1021/ar50139a006)
28. R. R. Holmes, in *Progress in Inorganic Chemistry*, S. J. Lippard, Ed., Wiley, New York, 2007, pp. 119–235 (https://doi.org/10.1002/9780470166338.ch2)
29. M. Pinsky, D. Avnir, *Inorg. Chem.* **37** (1998) 5575 (https://doi.org/doi.org/10.1021/ic9804925)
30. D. Casanova, J. Cirera, M. Llunell, P. Alemany, D. Avnir, S. Alvarez, *J. Am. Chem. Soc.* **126** (2004) 1755 (https://doi.org/10.1021/ja036479n)
31. Lj. S. Vojinović-Ješić, M. M. Radanović, *Coordination chemistry of aminoguanidine and its Schiff bases*, Faculty of Sciences, Novi Sad, 2017 (https://www.pmf.uns.ac.rs/wp-content/uploads/2016/04/vojinovicjesic_radanovic_koordinaciona_hemija_aminogvanidina.pdf) (in Serbian)
32. M. M. Belmonte, E. C. Escudero-Adán, E. Martin, A. W. Kleij, *Dalton Trans.* **41** (2012) 5193 (https://doi.org/10.1039/C2DT30201B)
33. S. P. Thomas, P. R. Spackman, D. Jayatilaka, M. A. Spackman, *J. Chem. Theory Comput.* **14** (2018) 1614 (https://doi.org/10.1021/ACS.JCTC.7B01200)
34. M. C. Etter, J. C. MacDonald, J. Bernstein, *Acta Cryst. B Struct. Sci. Cryst. Eng. Mater.* **46** (1990) 256 (https://doi.org/10.1107/S0108768189012929).